Raylike Structures in the Solar Corona

Shadia Rifai Habbal[1], Kenneth Wood[1], Richard Woo[2]

Received _____; accepted _____

[1]Smithsonian Astrophysical Observatory, 60 Garden Street, Cambridge, MA 02138; shabbal@cfa.harvard.edu; kenny@claymore.harvard.edu

[2]JPL/Caltech, 4800 Oak Grove Dr., Pasadena, CA 91109

ABSTRACT

Recent white light images from the large-angle spectroscopic coronagraph (LASCO) on the *Solar and Heliospheric Observatory* (SoHO) have revealed almost radially extending coronal structures out to several solar radii which fill the corona at all latitudes, except when they are overshadowed by streamers. We demonstrate in this *Letter* that the ubiquitous raylike structures observed in white light images of the corona are not limited to coronal holes and their boundaries. They naturally arise from line of sight integrations of the electron-scattered solar radiation when the three dimensional structure of a corona filled with open field lines having different densities is considered.

Subject headings: Sun: corona

1. Introduction

Wispy filamentary structures permeating the solar corona have always been one of the striking features of white light eclipse images (e.g. Koutchmy 1977). Known as polar plumes or polar rays, the origin of these structures is still the object of considerable debate. Because they are mostly visible in the inner corona in polar coronal holes, they have been attributed to unipolar field lines originating within the holes or at their boundaries (e.g. Saito 1965, Newkirk and Harvey 1968, Fisher and Guhathakurta 1995, Lamy et al. 1997). The association of these structures with the solar wind flow has been the subject of a number of investigations, with sometimes conflicting conclusions (compare, e.g., Ahmad and Withbroe 1977, Ahmad and Webb 1978, Walker et al. 1993, Habbal et al. 1995, DeForest et al 1997, Hassler et al. 1997).

The recent white light images from the LASCO C2 and C3 coronagraphs (Brueckner et al. 1995) revealed that not only do these coronal structures extend out to several solar radii, but they also fill the corona at all latitudes, except when they are overshadowed by streamers (see Figure 1). The extension of these raylike structures beyond 20 $R_\odot$ was discovered by radio occultation measurements (Woo 1996, Woo and Habbal 1997). Woo and Habbal (1997) and Habbal et al. (1997) showed that these raylike structures carried the fast solar wind and originated from coronal holes, their boundaries, as well as from quiet regions which cover the bulk of the solar disk.

The purpose of this *Letter* is to demonstrate that the ubiquitous raylike structures observed in white light images of the corona are not limited to coronal holes and their boundaries. They naturally arise from line of sight integrations of the electron-scattered solar radiation when the three dimensional structure of a corona filled with open field lines having different densities is considered.

2. Producing Images

To produce electron-scattered white-light images of the corona, we have developed a code which sets up the coronal electron density in a three dimensional regularly spaced cartesian grid. In the examples presented here, the grid extends to $\pm 6 R_\odot$ and has a total of eight million cells. Since the corona is optically thin to electron scattering (typical number densities are $n_e \sim 10^8 \mathrm{cm}^{-3}$ at $1 R_\odot$ in polar coronal holes), we assume that white light images arise from single Thomson scattering of solar radiation in the corona. We then make coronal white light images by performing line of sight integrations through our density grid of the source function for single Thomson scattering. This source function comprises the Thomson scattering phase function, the electron number density, and a geometrical term that describes the magnitude of the solar flux at any location in the corona. To compare our models with LASCO C2 images (e.g. Figure 1) we have introduced a "coronal mask" that is zero within $2 R_\odot$ and increases as r^2 outside the mask to simulate the graded filter response used for making coronal observations. In the following sections we show examples of white light images obtained for various coronal density structures.

3. Coronal Models

For illustrative purposes, we assume, throughout our modeling, that the electron density within either the corona n_c or a coronal hole n_h is purely radial, falling off as $1/r^2$, and that $n_c = 20 n_h$. We then modify this simple spherically symmetric model as follows:

3.1. Conical Coronal Holes

In the basic model shown in Figure 2, the density structure has n_c everywhere below latitudes $\pm\theta_H$ (with $\theta_H = 60°$). Above these latitudes the coronal hole density is given by

n_h. Thus at a height $|z|$ in the corona the cylindrical radius of the hole is defined by

$$\varpi_H = |z| \tan\theta_H \ . \tag{1}$$

As evident in Figure 2, bright radial structures arising from line of sight scattering effects reveal the boundaries of the coronal holes.

3.2. Non-axisymmetric Coronal Holes

Since coronal hole boundaries as observed on the disk, for example from the He I 10830 Å line, are far from rotationally symmetric, we constructed polar coronal holes with a sinusoidal boundary. At height $|z|$ in the corona, the cylindrical radius of the coronal hole boundary then varies with azimuthal angle, ϕ, as

$$\varpi_H = |z| \tan\theta_H \frac{1}{2}(1 + f + (1 - f)\sin m\phi) \ , \tag{2}$$

where f sets the amplitude and m is the number of "waves" in the coronal hole boundary. The electron density is n_h within this radius and n_c elsewhere.

Figure 3a shows the resulting scattered light images for coronal holes with $\theta_H = 60°$, $f = 0.25$ and $m = 8$. The four different viewing angles, separated by 30° in longitude, demonstrate the line of sight effects. While at one orientation the sinusoidal boundary results in prominent radial structures (see panels 2 and 4 in Figure 3a), at another orientation line of sight effects yield a scattered light image similar to Figure 2 (see panels 1 and 3 in Figure 3a). Due to the symmetry of the sinusoidal boundary, panels 1 and 3, 2 and 4, yield similar images in this example.

3.3. Mini Coronal Holes and Dense Tubes

Having demonstrated that line of sight effects can give rise to apparent radial structures within the boundaries of polar coronal holes, we investigated what would be the effect of many mini radial coronal holes that fill the corona and also denser tubes within coronal holes. We chose random locations on the solar surface between latitudes $\pm\theta_H$ for the origins of the mini coronal holes and above $\pm\theta_H$ for the dense tubes. The mini holes and tubes are all assumed to form radial structures with diameters chosen randomly to be between 5° and 10°. Within the mini holes the electron density is n_h and the dense tubes in the polar coronal holes have density $2n_h$.

Figure 3b shows the results of a simulation where we have randomly placed 200 radial mini holes (100 in each hemisphere), and eight dense tubes in the coronal holes (four in each polar hole) in the same coronal hole boundary configuration as Figure 3a. This image shows many bright and dark raylike structures filling the corona. The dark structures are formed by mini holes along the line of sight, while the bright structures arise from electron scattering in the corona. Some of the bright structures appear to be very narrow along lines of sight where mini holes lie very close to each other giving the illusion of a bright dense stalk. Such bright structures may be formed by scattering in a denser coronal stalk, but clearly scattered white light images alone cannot distinguish between dense stalks and the line of sight effect of closely spaced mini holes. The radial raylike structures move in latitude as the model corona is viewed at different rotational phases. This "searchlight" effect is also seen in LASCO C2 movies.

3.4. Current Sheets

Our final model comprises the same ingredients of Figure 3b with the addition of a radially extending current sheet with a density of $5n_c$. We assume that between longitudes 0°-180° the current sheet has a sinusoidal structure and extends radially with a thickness of 4°. Between 180°-360° the current sheet lies between latitudes ±2°. Figure 3c shows the resulting images for this density structure. This particular form for the current sheet yields equatorial radial structures that change with viewing angle. At some orientations there appears to be a single radial structure on the west and a two-pronged structure on the east (e.g. Figure 1c-3c). Again this arises purely from line of sight scattering effects as demonstrated by Wang et al. (1997).

4. Discussion and Conclusions

Starting from the observation that the origin of the fast solar wind appears to be from polar coronal holes and that open field lines fill the quiet regions, we have made model white light images for different coronal densities. In our simple model we assume that all open field lines extend purely radially. We find that line of sight scattering effects naturally lead to the formation of many raylike structures with a remarkable resemblance to the LASCO C2 images.

In polar coronal holes, the radial extension of a non-axisymmetric boundary, as found by Woo and Habbal (1997) and Woo et al. (1998), leads to the impression of a well-defined boundary, in addition to bright and dark raylike structures within the coronal hole itself. However, to reproduce the abundance of raylike structure observed in the corona, additional flow tubes are needed both within the coronal holes and in the neighboring quiet regions. When many flow tubes with depressed densities compared to their surroundings are

included in the quiet regions the scattered light images show a plethora of bright and dark structures. The bright rays are a consequence of the contrast produced when lower density flow tubes lie close to one another along the same line of sight. We also note here that the same contrast can be achieved with flow tubes in the quiet regions being denser than their surroundings.

Included in this study are only radially extended structures. The tilt angle of the rotation axis with respect to the ecliptic has not been factored into the calculations, neither have the closed field line regions forming the bulge of the streamers. However, the results clearly illustrate that the preponderance of raylike structures in the corona, as observed in the LASCO C2 images can be readily accounted for by a preponderance of radially extending flow tubes originating from a large fraction of the solar surface, in both coronal holes and quiet regions. In particular, these results demonstrate that open field lines must abound in quiet regions. However, it is not necessary that all field lines be radially aligned. But there is no evidence in either the observations or the modeling for a significantly strong divergence of the flow tubes beyond radial as is commonly assumed for the boundaries of polar coronal holes (e.g. Zirker 1977).

This simple model has qualitatively demonstrated that open field lines with different densities covering a significant fraction of quiet regions and coronal holes, lead to the observed coronal raylike structures.

This work was supported by the National Aeronautics and Space Administration (NASA) under grants NAG5-6215 (SRH), NAG5-6039 (KW) from NASA's Long Term Space Astrophysics Research Program, and under a contract with NASA to the Jet Propulsion Laboratory, California Institute of Technology (RW).

References

Ahmad, I. A. and Webb, D. F. 1978, Sol. Phys., 58, 323

Ahmad, I. A. and Withbroe, G. L. 1977, Sol. Phys., 53, 397

Brueckner, G. E., et al. 1995, Sol. Phys., 162, 357

DeForest, C. E., et al. 1997, Sol. Phys., 175, 393

Fisher, R. and Guhathakurta, M. 1995, ApJ, 447, L139

Habbal, S. R. et al. 1995, Geophys. Res. Lett., 22. 1465

Habbal, S. R. et al. 1997, ApJ, 489, L103

Hassler, D. M. et al. 1997, Sol. Phys., 175, 375

Kohl, J. L. et al. 1995, Sol. Phys., 162, 313

Koutchmy, S. 1977, Sol. Phys., 51, 399

Lamy, P. et al. 1997, in *Proceedings of the SOHO 5 Workshop*, ESA SP-404, 487

Newkirk, G., Jr. and Harvey, J. 1968, Sol. Phys., 3, 321

Saito, K. 1965, Publ. Astron. Soc. Japan, 17, 1

Walker, A. B. C. et al., 1993, Sol. Phys., 148, 239

Wang, Y.-M., et al. 1997, ApJ, 485, 889

Woo, R. 1996, ApJ, 464, L95

Woo, R. and Habbal, S. R. 1997, Geophys. Res. Lett., 24, 1159

Woo, R. et al. 1998, submitted to ApJ

Zirker, J. B., (Ed.) Coronal Holes and High Speed Wind Streams, 1977, Colorado

Associated University Press.

Figure Captions

Figure 1. A composite image of the corona made on 15 August 1996, with X-ray emission (red disk) from Yohkoh, with polarized brightness from Mauna Loa MkIII coronagraph between 1.15 to 1.75 $R_\odot$, and with white light emission beyond 2 $R_\odot$ using the LASCO C2 coronagraph.

Figure 2. Model image of the white light corona for a spherically symmetric corona and coronal hole boundaries at $\pm\theta_H = 60°$.

Figure 3. Model images of a white light corona for (a) polar coronal holes with a sinusoidal boundary, and with (b) an additional random distribution of 200 radially expanding flow tubes with different densities in coronal holes and quiet regions, and with (c) a non sphericallly symmetric current sheet, for viewing angles differing by 30° (panels 1-4).

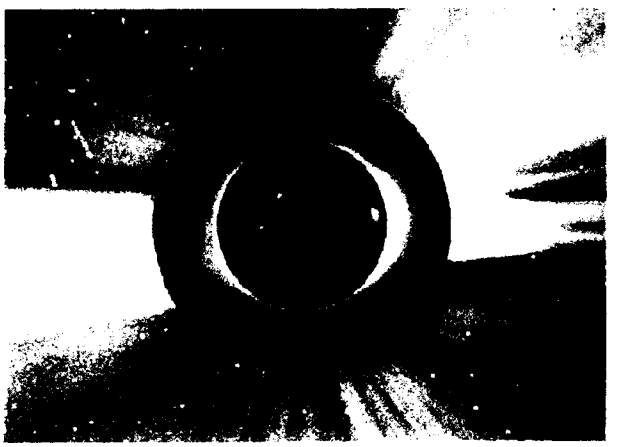

FIG.1

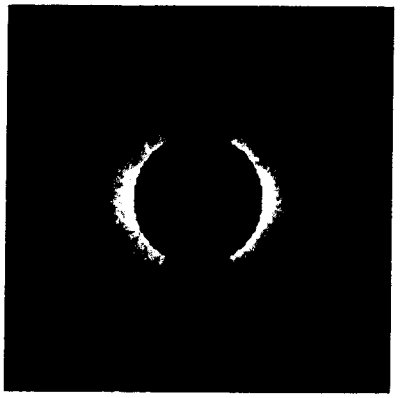

FIG. 2

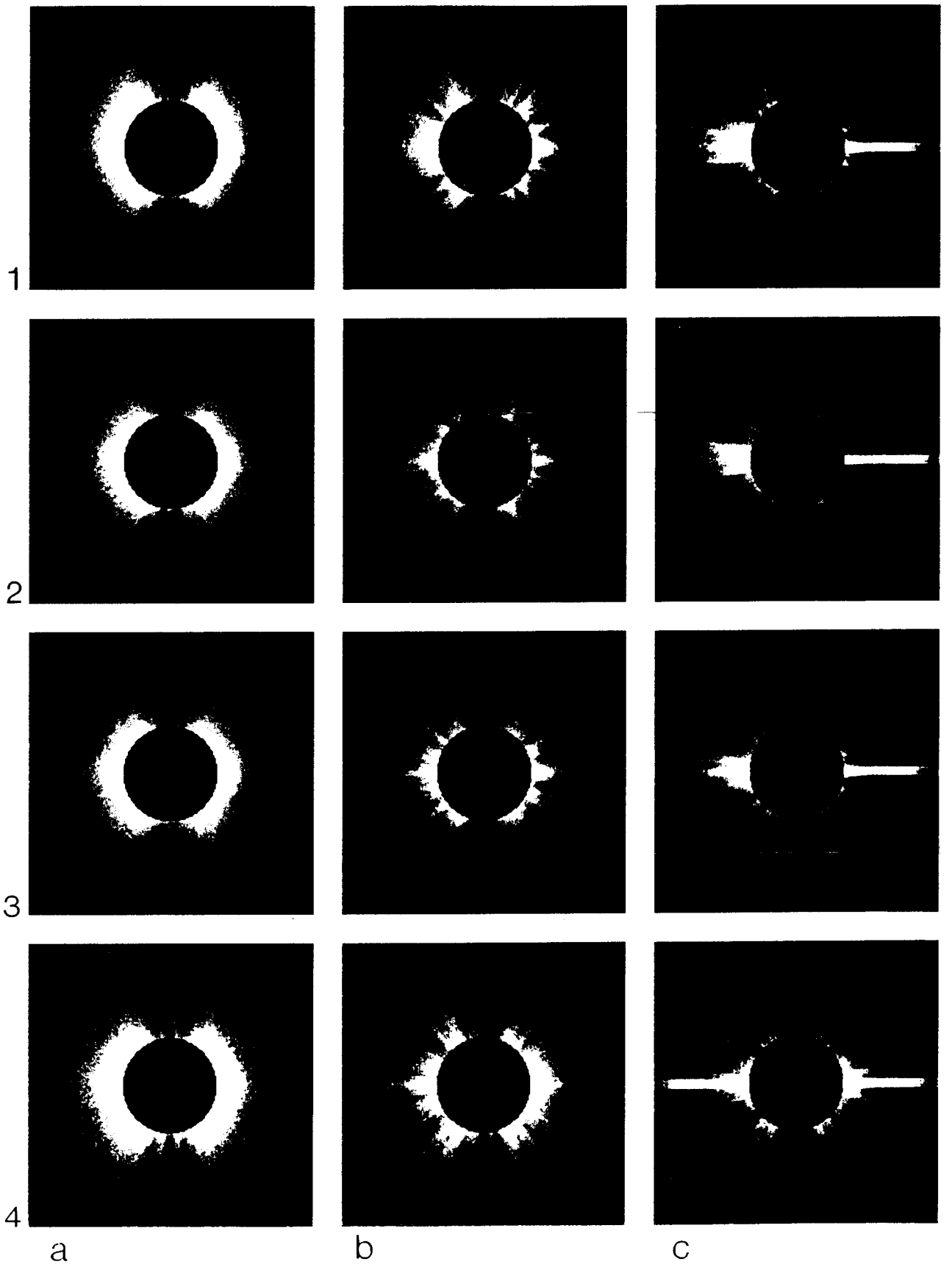

FIG 3